Leaf chlorophyll content as a proxy for leaf photosynthetic capacity

HOLLY CROFT[1], JING M. CHEN[1], XIANGZHONG LUO[1], PAUL BARTLETT[2], BIN CHEN[1,3] and RAL F M. STAEBLER[4]

[1] University of Toronto, Department of Geography, Toronto, ON M5S 3G3, Canada, [2] Climate Research Division, Environment and Climate Change Canada, Toronto, ON, Canada, [3] International Institute for Earth System Science, Nanjing University, Nanjing, China, [4] Air Quality Processes Research Section, Environment and Climate Change Canada, 4905 Dufferin Street, Toronto, ON M3H 5T4, Canada

Abstract

Improving the accuracy of estimates of forest carbon exchange is a central priority for understanding ecosystem response to increased atmospheric CO_2 levels and improving carbon cycle modelling. However, the spatially continuous parameterization of photosynthetic capacity (Vcmax) at global scales and appropriate temporal intervals within terrestrial biosphere models (TBMs) remains unresolved. This research investigates the use of biochemical parameters for modelling leaf photosynthetic capacity within a deciduous forest. Particular attention is given to the impacts of seasonality on both leaf biophysical variables and physiological processes, and their interdependent relationships. Four deciduous tree species were sampled across three growing seasons (2013–2015), approximately every 10 days for leaf chlorophyll content (Chl_{Leaf}) and canopy structure. Leaf nitrogen (N_{Area}) was also measured during 2014. Leaf photosynthesis was measured during 2014–2015 using a Li-6400 gas-exchange system, with A-Ci curves to model Vcmax. Results showed that seasonality and variations between species resulted in weak relationships between Vcmax normalized to 25°C ($Vcmax_{25}$) and N_{Area} ($R^2 = 0.62$, $P < 0.001$), whereas Chl_{Leaf} demonstrated a much stronger correlation with $Vcmax_{25}$ ($R^2 = 0.78$, $P < 0.001$). The relationship between Chl_{Leaf} and N_{Area} was also weak ($R^2 = 0.47$, $P < 0.001$), possibly due to the dynamic partitioning of nitrogen, between and within photosynthetic and nonphotosynthetic fractions. The spatial and temporal variability of $Vcmax_{25}$ was mapped using Landsat TM/ETM satellite data across the forest site, using physical models to derive Chl_{Leaf}. TBMs largely treat photosynthetic parameters as either fixed constants or varying according to leaf nitrogen content. This research challenges assumptions that simple N_{Area}–$Vcmax_{25}$ relationships can reliably be used to constrain photosynthetic capacity in TBMs, even within the same plant functional type. It is suggested that Chl_{Leaf} provides a more accurate, direct proxy for $Vcmax_{25}$ and is also more easily retrievable from satellite data. These results have important implications for carbon modelling within deciduous ecosystems.

Keywords: carbon cycle, ecosystem modelling, Jmax, leaf nitrogen, remote sensing, Vcmax

Introduction

There is currently considerable uncertainty in the nature of the sinks, sources and distribution of carbon exchange between the atmosphere and the terrestrial biosphere (IPCC 2013; Brienen *et al*., 2015). Land–atmosphere CO_2 exchange varies nonlinearly in response to a range of biotic and abiotic drivers, hampering modelling efforts, both under current conditions and also for future projections. Forests are estimated to contain a net global forest carbon sink of 1.1 (±0.8) Pg C $year^{-1}$ (Pan *et al*., 2011), which resides predominantly in temperate and boreal forests, and represents an important part of the global carbon cycle. Photosynthesis facilitates 90% of carbon and water fluxes within the biosphere–atmosphere system (Joiner *et al*., 2011), through the conversion of solar radiation into chemical energy. However, plant photosynthetic rates respond quickly to changes in environmental conditions, causing rates to be highly variable even at annual timescales, and its behaviour difficult to forecast in the light of a changing climate (IPCC 2013). The importance of photosynthetic carbon uptake to carbon budgets has made photosynthesis rates a key source of uncertainty in modelling the global carbon cycle, due to the difficulty in providing accurate estimates over large spatial extents.

Terrestrial biosphere models (TBMs) are the principal means for providing regional and global estimates of terrestrial carbon cycling (Beer *et al*., 2010). TBMs typically include a photosynthesis scheme using an enzyme kinetic model developed by Farquhar *et al*. (1980), according to the parameterization of atmospheric CO_2 concentration, photosynthetic capacity and leaf temperature (Kattge *et al*., 2009). Photosynthetic capacity is defined in terms of the maximum rate of carboxylation (Vcmax) and the maximum rate of electron transport (Jmax). Vcmax describes the intrinsic photosynthetic capacity of the leaf, according to the amount, activity and kinetics of the RuBisCo (ribulose 1,5-bisphosphate carboxylase/oxygenase) enzyme (Grassi *et al*., 2005). Jmax determines the rate of Ribulose 1,5-bisphosphate (RuBP) regeneration, via the electron transport chain (von Caemmerer & Farquhar, 1981; Sharkey *et al*., 2007). A large source of uncertainty in modelled carbon predictions arises from the sensitivity of photosynthesis rates to leaf photosynthetic capacity. Additionally, research has shown that Vcmax varies considerably within and between vegetation species, according to environmental controls (Xu & Baldocchi, 2003; Groenendijk *et al*., 2011). Despite this sensitivity of photosynthesis rates to leaf photosynthetic capacity, most models assume a fixed Vcmax value (normalized to 25°C; V_{cmax25}) over time, according to plant functional type (PFT) (Zhang *et al*., 2014). However, for the same PFT, V_{cmax25} can vary by a factor of 2–3, causing large errors in modelled photosynthesis estimates, particularly for regions or ecosystems with a large seasonal range (e.g. deciduous forests) or in areas prone to drought (Grassi *et al*., 2005; Dillen *et al*., 2012; Medvigy *et al*., 2013). Progress in using accurate photosynthetic capacity values within TBMs has largely been hindered by the difficulty in

obtaining spatially continuous V_{cmax25} values at global scales (Kattge *et al*., 2009). Direct retrievals of Vcmax, through gas-exchange measurements, are time-consuming and restricted to the leaf scale, which ultimately results in a relative paucity of measured data over a complete range of species and environmental conditions. At the canopy scale, Vcmax is more commonly modelled from eddy covariance flux measurements and meteorological data (Wang *et al*., 2007).

To avoid using a fixed constant for V_{cmax25}, a common approach is to exploit relationships between more easily measurable plant functional traits (e.g. leaf phosphorus, leaf nitrogen (N_{Leaf}), specific leaf area (SLA)) and photosynthetic capacity (Walker *et al*., 2014). Thus far, most interest has focused on N_{Leaf} (Kattge *et al*., 2009), because nitrogen is a major constituent of RuBisCo and the light-harvesting complexes that also modulate photosynthesis (Niinemets & Tenhunen, 1997). TBMs therefore often parameterize Vcmax according to predefined relationships with N_{Leaf}, for a given PFT (Dietze, 2014). However, retrieving N_{Leaf} over large spatial scales has proved complex (Knyazikhin *et al*., 2013). In contrast, there has been relatively little research into relationships between photosynthetic capacity and other biochemical photosynthetic components, such as leaf chlorophyll (Chl_{Leaf}) or carotenoid content, in the context of process-based ecosystem modelling. Chlorophyll is responsible for light harvesting in photosynthesis, resulting in the excitation of electrons that are used to drive the production of nicotinamide adenine dinucleotide phosphate (NADPH) and chemical energy in the form of adenosine triphosphate (ATP), for the reactions of the Calvin–Benson cycle. Houborg *et al*. (2013) used semi-empirical relationships to model V_{cmax} from chlorophyll, according to the fraction of leaf nitrogen in RuBisCo as an intermediary. Dillen *et al*. (2012) showed a correlation between a spectral reflectance index (λRE) sensitive to chlorophyll content and Vcmax at a deciduous forest. Other studies have related Chl_{Leaf} to vegetation productivity using light use efficiency (LUE)-based approaches (Gitelson *et al*., 2006; Croft *et al*., 2015a; Schull *et al*., 2015). The strong correlation that has been reported between Chl_{Leaf} and N_{Leaf} (Sage *et al*., 1987) has also lead to suggestions that Chl_{Leaf} can be used as an operational proxy for N_{Leaf} (and thus V_{cmax25}) (Homolova *et al*., 2013).

Remotely sensed data offer the unique potential of deriving spatially continuous plant physiological information at global scales (Hilker *et al*., 2008). Previous efforts using remote sensing products to improve modelled estimates of carbon fluxes from terrestrial ecosystems have focussed on using vegetation indices such as the biomass-sensitive NDVI or EVI as indicators of canopy greenness (Turner *et al*., 2003) or using imaging spectroscopy to map foliar traits (Serbin *et al*., 2015). Efforts to map Vcmax directly are less well-developed, although promising new research has demonstrated the potential of solar-induced fluorescence for such purposes, using sensors such as GOME-2 (Zhang *et al*., 2014). However, these measurements are only available at a restrictively coarse spatial resolution

(40 × 80 km^2). Direct retrievals of photosynthetic capacity from optical remote sensing data based on sound underlying mechanical principles are still emerging. This research aims to investigate the potential of leaf biochemistry at leaf and canopy levels to produce spatially continuous maps of key photosynthetic parameters for improved ecosystem modelling. The specific objectives of the research were to 1) examine the relationship between photosynthetic capacity with Chl_{Leaf} and N_{Leaf} in a temperate deciduous forest and 2) assess the suitability of using Chl_{Leaf} and N_{Leaf} to derive Vcmax over large spatial scales from remote sensing data.

Materials and methods

Field site description

The Borden Forest Research Station is a mixed temperate forest located in southern Ontario (44°19′N, 79°56′W) within the Great Lakes/St. Lawrence forest region (Froelich *et al*., 2015). This ecotone extends across eastern North America between 44 and 47° N and represents a region of ecological importance. It is a transition zone between southern temperate forest species and northern boreal species, and has been identified as susceptible to environmental change through northward migrations of tree species (Leithead *et al*., 2010). The mean annual temperature at the site is approximately 7.4°C, and mean annual total precipitation is 784 mm (Froelich *et al*., 2015). The mean canopy height is 22 m, with dominant species including red maple (*Acer rubrum*), eastern white pine (*Pinus strobus*), bigtooth aspen and trembling aspen (*Populus grandidentata* and *Populus tremuloides*) and white ash (*Fraxinus americana*) (Lee *et al*., 1999; Teklemariam *et al*., 2009).

Leaf biochemistry and leaf area index measurements

Leaves were sampled from the upper canopy of four tree species (red maple, bigtooth aspen, trembling aspen and white ash), directly from a 44-m flux tower located at the site. From each species, five leaves were sampled approximately every 10 days during the 2013–2015 growing seasons for biochemical analysis. The sampled branches were tagged to ensure repeatable measurements through the growing season. Leaf samples were sealed in plastic bags and kept at a temperature of 0°C for subsequent biochemical analysis to extract Chl_{Leaf}. Foliar chlorophyll was extracted using spectra-analysed grade *N,N*-dimethylformamide, and absorbance was measured at 663.8, 646.8 and 480 nm using a Shimadzu UV-1700 spectrophotometer (Wellburn, 1994; Croft *et al*., 2013, 2014a). The measured Chl_{Leaf} values for each species were calculated as mean values from the five leaf samples per species collected on each sampling date. As Chl_{Leaf} was measured from leaves sampled from the top of the canopy, values represent the maximum leaf chlorophyll potential for a given date leaves (Zhang *et al*., 2007). Nitrogen content was also measured on the same leaf samples as used for Chl_{Leaf} determination during the 2014 season. Leaf samples were dried at 80°C for 48 h, ground to a powder using a Wiley mill

and analysed on an ECS 4010 Elemental Combustion System for CHNS-O analysis (Costech Analytical Technologies, Valencia, California).

Leaf area index (LAI) and canopy structural parameters were measured on the same days as leaf sampling. Effective LAI (*L*e) measurements were obtained using the LAI-2000 plant canopy analyser (Li-Cor, Lincoln, NE, USA), following the methods outlined by Chen *et al*. (1997), and converted to true LAI values as follows:

$$\mathrm{LAI} = [(1 - \alpha)Le\gamma_E]/\Omega \quad (1)$$

where α is the ratio of woody area to total area, γ_E is the ratio of needle area to shoot area, and Ω is the clumping index. The ratio of woody area to total area (α = 0.17) accounts for the interception of radiation by branches and tree trunks that results in artificially high LAI values and was obtained from the previously published values of similar deciduous stands (Gower *et al*., 1999). For broadleaf species, individual leaves are considered foliage elements and γ_E is set at 1. The element clumping index (Ω_E) was measured using the TRAC (Tracing Radiation and Architecture of Canopies) instrument (Chen & Cihlar, 1995). Midseason Ω_E values derived from TRAC ground measurements were typically circa 0.96. LAI-2000 and TRAC measurements were collected along a 100-m transect at 10-m intervals, extending from the flux tower in a north–south orientation.

Gas-exchange measurements and photosynthetic parameters

Field measurements of leaf-level gas exchange were carried out using the LI-6400 portable infrared gas analyzer (LI-COR, Lincoln, NE, USA) during the complete growing seasons of 2014 and 2015, immediately following budburst until leaf fall. Measurements were taken on the same day as field sampling for leaf biochemistry and LAI. Leaves from all four species were selected from the same top-of-canopy branches as the leaf samples used for chlorophyll and nitrogen analysis, and where possible repeat measurements of the same leaf were taken throughout the growing season. The LI-6400 was fitted with a 6400-02B Red/Blue Light Source, and CO_2 response curves (A–Ci curves) were produced under light-saturating conditions, at photosynthetic photon flux density (PPFD) levels of 1800 μmol m^{-2} s^{-1}, and stepwise CO_2 concentrations of 400, 200, 100, 50, 400, 600, 800, 1000, 1200, 1500, 1800 μmol CO_2 mol^{-1} air. Prior to logging measurements, leaves acclimated in the chamber at 1800 μmol m^{-2} s^{-1}, ambient relative humidity, a temperature of 25°C and a CO_2 concentration of 400 μmol CO_2 mol^{-1} air. Throughout the measurement sequence, the leaf chamber was maintained as close to 25°C as possible (approximately ±1°C) and relative humidity kept between 40% and 80%. A complete *A*/*C*i response curve took approximately 1 h to carry out. The photosynthetic parameters Vcmax and Jmax were calculated from the A-Ci curves fitted using a curve-fitting tool developed by Kevin Tu (www.landflux.org) following Ethier & Livingston (2004) to the Farquhar biochemical model of leaf photosynthesis (Farquhar *et al*., 1980). The fitted Vcmax and Jmax parameters were scaled to a common reference

temperature of 25°C using the Arrhenius equation to facilitate comparability amongst existing data sets (Sharkey *et al*., 2007; Sharkey, 2016).

Satellite processing and leaf chlorophyll retrieval algorithm

Cloud-free Landsat-5 TM, -7 ETM and -8 OLI atmospherically corrected reflectance products were obtained for the years 2013–2015. Scenes with missing data over the site resulting from the Landsat 7 ETM Scan Line Corrector (SLC) malfunction were not used in the analysis. From the Landsat canopy-level reflectance, foliar chlorophyll content was modelled using a canopy geometrical–optical model (Chen & Leblanc, 1997) linked with a leaf radiative transfer model (Jacquemoud & Baret, 1990), according to the algorithm detailed in Croft *et al*. (2013). The 4-scale model simulates the bidirectional reflectance distribution function (BRDF) based on canopy architecture at four scales: (1) tree groups, (2) tree crown geometry, (3) branches, and (4) foliage elements (Chen & Leblanc, 2001). A crown is represented as a complex medium, where reflected radiance from shaded components is determined by first-order scattering (separating sunlit and shaded components), and multiple scattering from subsequent interactions with vegetation or background material (Chen & Leblanc, 2001). The four-scale model was run in the forward mode, using fixed and variable structural parameters and leaf and understory reflectance spectra to model canopy reflectance and inverted using a look-up-table (LUT) approach (Zhang *et al*., 2008; Croft *et al*., 2013). To model spatially leaf chlorophyll content over larger spatial extents, LAI was derived empirically using the normalized difference vegetation index (NDVI), according to relationships with ground measurements of LAI taken across the growing season (Fig. 1).

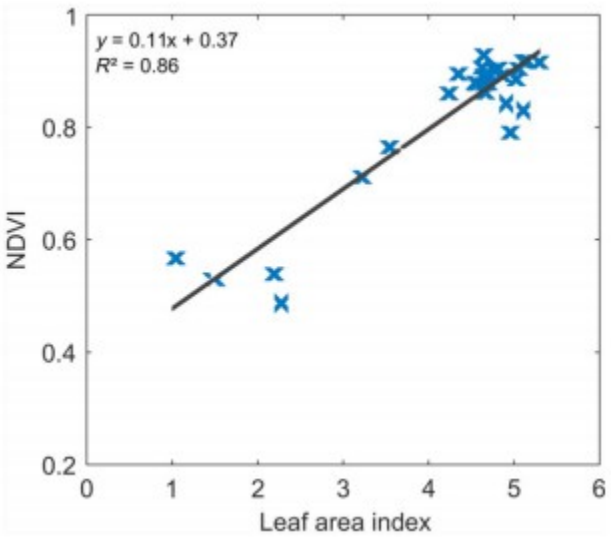

FIGURE 1 Regression between Landsat-derived NDVI and measured leaf area index

The leaf radiative transfer model PROSPECT (Jacquemoud & Baret, 1990) was then used to model leaf chlorophyll content using the derived leaf reflectance spectra. Leaf optical properties (reflectance and transmittance)

from 400 to 2500 nm are defined in PROSPECT5 as a function of six parameters: structure parameter (N), chlorophyll (a + b) concentration, dry matter, water content, carotenoid content and a brown pigment parameter to represent nonphotosynthetic leaf matter. Absorption is calculated as the linear summation of the specific absorption coefficients of biochemical constituents and their respective concentrations. The absorption coefficients were recalculated to the corresponding Landsat bands using their respective spectral response functions. PROSPECT has previously been successfully used to model chlorophyll from multispectral data (Croft *et al*., 2015b).

Results

Seasonal variation in leaf biochemistry and photosynthetic processes

Temperate deciduous forests exhibit considerable temporal variation in both biochemical and structural attributes, and also physiological processes throughout the growing season. Understanding the nature of these relationships is vital for accurately modelling carbon exchange in deciduous ecosystems. Figure 2 shows the large seasonal variations in several important leaf biophysical properties and photosynthetic processes during 2014, along with the variability that exists between species, even within the same functional type. Trembling and bigtooth aspen both displayed markedly higher chlorophyll and nitrogen values than red maple and ash, in addition to higher V_{cmax25} and J_{max25} values. Lower SLA values can result in a lower leaf photosynthetic potential per area dry mass, but are compensated by increased leaf structural strength (Niinemets & Sack, 2006). However, these results show that leaf photosynthesis and stomatal conductance were also dominated by high bigtooth aspen values, despite the lower SLA, with red maple displaying the lowest values.

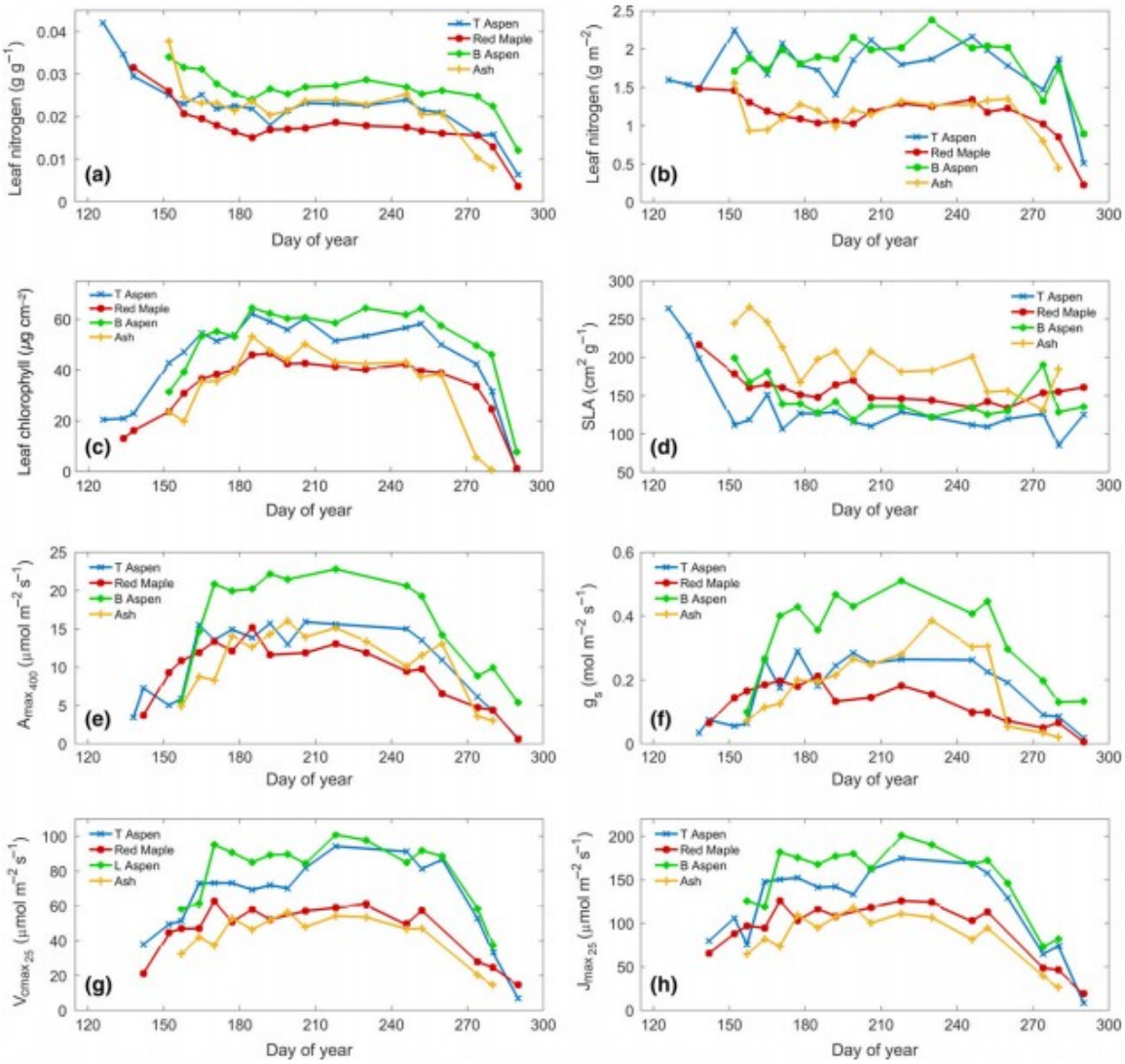

FIGURE 2 Seasonal variations in 2014 for (a) leaf nitrogen by mass (g g^{-1}), (b) leaf nitrogen by area (g m^{-2}); (c) leaf chlorophyll content (μg cm^{-2}), (d) specific leaf area (cm^2 g^{-1}), (e) maximum leaf photosynthesis at 400 ppm CO_2 (A_{max400}; μmol m^{-2} s^{-1}), (f) stomatal conductance (g_s; μmol m^{-2} s^{-1}), (g) V_{cmax25} (μmol m^{-2} s^{-1}), (h) J_{max25} (μmol m^{-2} s^{-1}), for all four measured species. T Aspen and B Aspen refer to trembling aspen and bigtooth aspen, respectively.

Leaf nitrogen is expressed on a mass (N_{Mass}; Fig. 2a) and area (N_{Area}; Fig. 2b) basis. N_{Mass} shows maximum values following budburst at the start of the season, following by stabilization in the middle of the growing season and a decline during leaf senescence. N_{Area} trends are adjusted according to variations in SLA, with higher SLA values at the start of the season compensating for the higher N_{Mass} values seen in early season. Notably, both N_{Mass} and N_{Area} are both high at the start of the season, relative to Chl_{Leaf} (Croft *et al.*, 2014ab; Croft *et al.*, 2015a). Photosynthesis rates display a similar seasonal profile to Chl_{Leaf}, increasing slowly at the start of the season, until values stabilize in the middle of the growing season, and declining during leaf senescence. As the leaf gas-exchange measurements were taken under

controlled, repeatable and stable conditions with the same irradiance levels (1800 µmol m^{-2} s^{-1}) and temperature (25°C ± 1°C), these results indicate that the low photosynthesis rates were due to undeveloped or broken down leaf photosynthetic apparatus in the spring and fall rather than unfavorable ambient environmental conditions.

Relationships between leaf nitrogen and leaf chlorophyll content

Considerable research has been devoted to exploring the relationships between N_{Leaf} and Chl_{Leaf} content to use Chl_{Leaf} as a proxy for N_{Leaf} which is in turn used to constrain V_{cmax25}. This approach is taken due to the difficulty in obtaining N_{Leaf} from remote sensing techniques (Knyazikhin *et al*., 2013), compared with chlorophyll content (Croft *et al*., 2013, 2014c), and is justified by the underlying investment of nitrogen in chlorophyll molecules. Whilst research has found linear relationships between N_{Leaf} and Chl_{Leaf} (Sage *et al*., 1987), little work has explored this relationship within a seasonal context (Fig. 3).

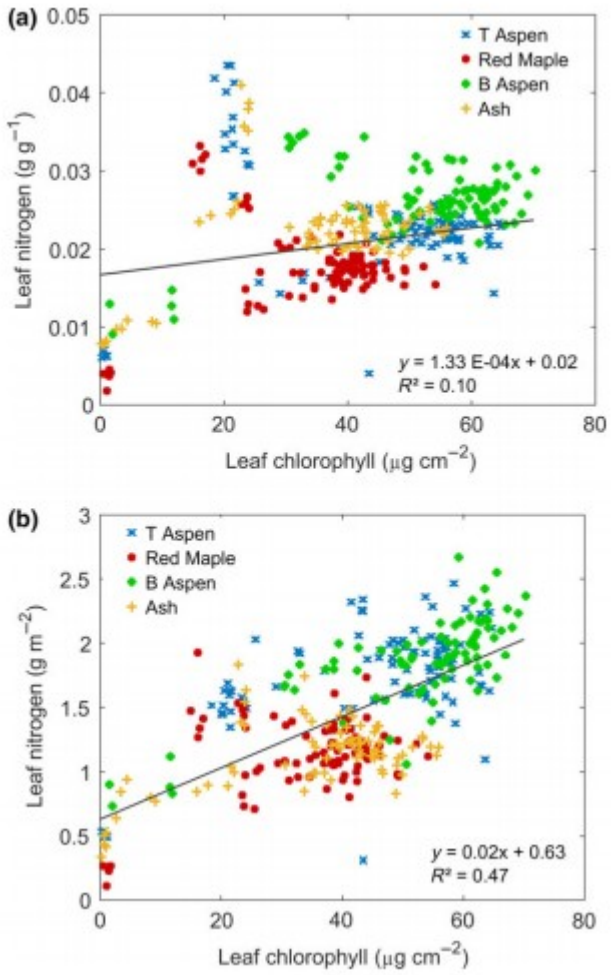

FIGURE 3 Relationships between (a) nitrogen by mass (g g^{-1}), $P < 0.001$, and (b) nitrogen by area (g m^{-2}), $P < 0.001$, with leaf chlorophyll content (µg cm^{-2}), for all four sampled tree species.

Figure 3 clearly demonstrates the variability in the relationship between Chl_{Leaf} and both N_{Mass} and N_{Area}. Figure 3a in particular shows the divergence of the two variables at the start and end of the growing season, where two separate clusters of nitrogen values are present; one is between 0.025 and 0.045 g g^{-1}, representing higher values than corresponding chlorophyll from early in the season. The second cluster is where Chl_{Leaf} is negligible during leaf senescence, but N_{Leaf} persists, likely due to investments in leaf structural components, such as cellulose. The adjustment by SLA to express nitrogen by area corrects for the start of season bias, but nitrogen is still higher than corresponding chlorophyll values at the end of the season. Figure 3 indicates the complexity in the relationship between total leaf nitrogen and leaf chlorophyll, with the partitioning of total N_{Leaf} between different nitrogen pools in the leaf, both dynamically across the growing season and according to tree species. This variability affects the overall relationship with Chl_{Leaf}, leading to weak relationships (R^2 = 0.10 and R^2 = 0.47, for N_{Mass} and N_{Area}, respectively).

The ratio between Chl_{Leaf} and N_{Area} (both expressed using the same μg cm^{-2} SI units) provides information on the allocation of nitrogen between photosynthetic proteins, such as RuBisCo and the chlorophyll light-harvesting pigments (Kenzo *et al*., 2006). Figure 4 shows the seasonal variations in the Chl_{Leaf}/N_{Area} ratio for all four tree species.

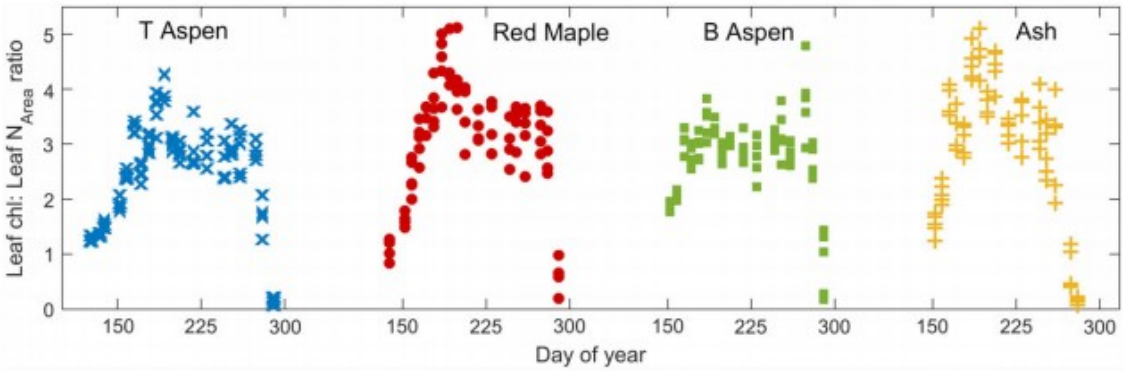

FIGURE 4 Variations in the leaf chlorophyll to leaf nitrogen ratio, across a growing season and between tree species.

Figure 4 shows the large seasonal variation in Chl_{Leaf}/N_{Area} ratios, with low values at the start of season, ranging from 0.8 for red maple to 1.2 for ash and trembling aspen. The midseason mean values (defined at the time period between asymptotes at DOY 178 and 274) were 3.8 for both ash and red maple, and 3.1 and 3.0 for trembling and bigtooth aspen, respectively. Ratios dropped at the end of the season following leaf senescence, as Chl_{Leaf} was broken down, but nitrogen pools remained in structural components of the leaf. The midseason variations between species are also noteworthy; the lower aspen Chl_{Leaf}/N_{Area} ratios were also matched by higher $Amax_{400}$ and $Vcmax_{25}$ values and higher Chl_{Leaf} and N_{Area} values (Fig. 2). This may indicate

that relatively more nitrogen is invested in RuBisCo than in the light-harvesting complexes in the aspen species, leading to increased photosynthetic capacity under certain environmental conditions. The temporal variability in the relationship in particular, but also the species-specific dependency, has important implications for remote sensing research that aims to use a straightforward relationship between N_{Leaf} and Chl_{Leaf} to use Chl_{Leaf} as a more reliable means of retrieving N_{Leaf}.

Leaf biochemistry and photosynthetic capacity

Due to the difficulty in measuring Vcmax and Jmax over broad spatial extents, parameterization within TBMs often assumes these values to be temporally invariant or they are calculated from more easily measurable parameters, most commonly leaf nitrogen content (Grassi *et al*., 2005). Figure 5 investigates the relationship between $Vcmax_{25}$ and $Jmax_{25}$ with both N_{Area} and Chl_{Leaf}.

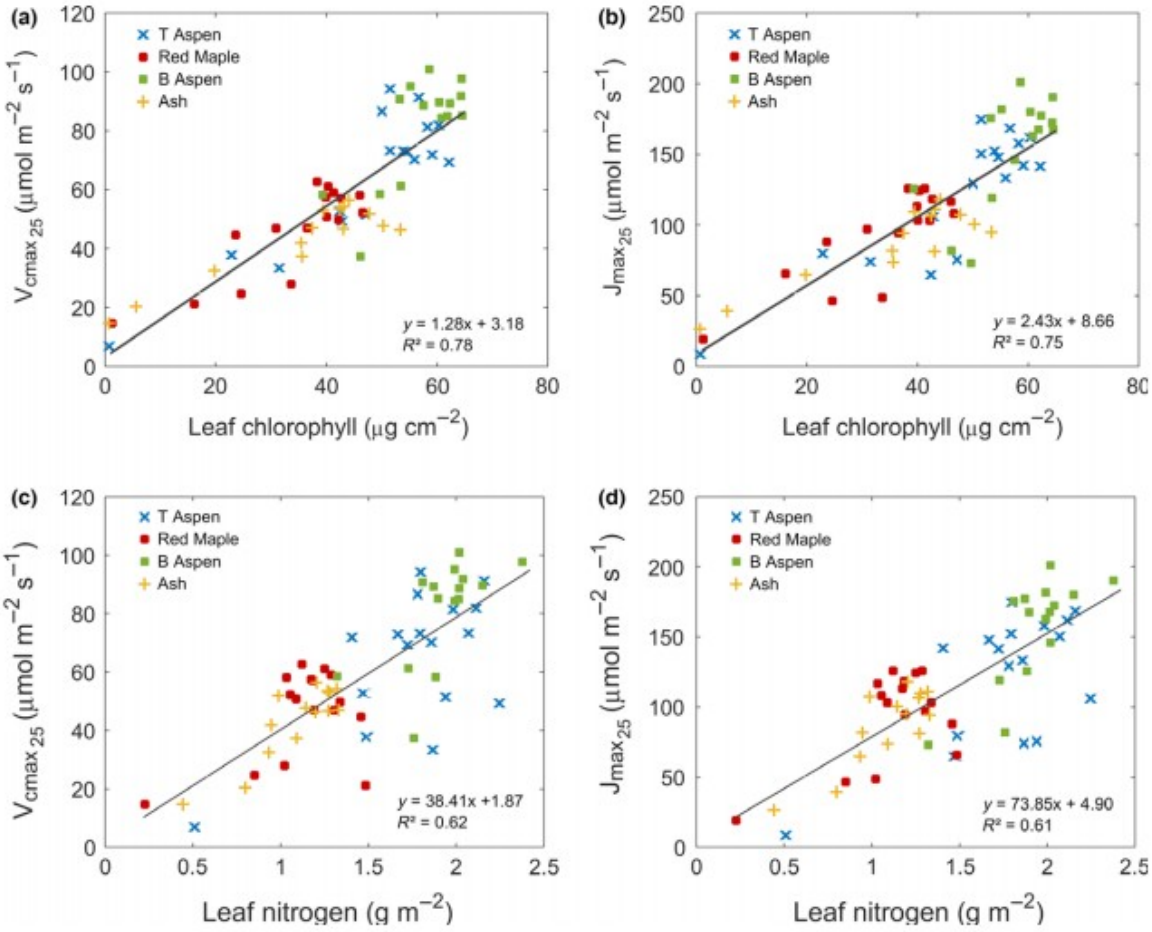

FIGURE 5 Relationships between leaf chlorophyll (µg cm^{-2}) and (a) $Vcmax_{25}$ (µmol m^{-2} s^{-1}); (b) $Jmax_{25}$ (µmol m^{-2} s^{-1}); and leaf nitrogen by area (g m^{-2}) and (c) $Vcmax_{25}$ (µmol m^{-2} s^{-1}); (d) $Jmax_{25}$ (µmol m^{-2} s^{-1}), where in all cases $P < 0.001$, for 2014 data.

The results in Fig. 5 show a strong relationship between Chl_{Leaf} and both $Vcmax_{25}$ ($R^2 = 0.78$, $P < 0.001$) and $Jmax_{25}$ ($R^2 = 0.75$, $P < 0.001$). However, the relationships between leaf nitrogen (area) and $Vcmax_{25}$ and $Jmax_{25}$ were weaker ($R^2 = 0.62$, $P < 0.001$ and $R^2 = 0.61$, $P < 0.001$, respectively). As with results presented in Fig. 3, this relationship is likely to be affected by the fraction of nitrogen invested in RuBisCo, the light-harvesting compounds and bioenergetic pathways, and also in the structural components of the leaf. It highlights the need for deriving function-specific nitrogen fractions rather than total nitrogen for modelling photosynthetic parameters, especially for use within TBMs that employ a nitrogen cycle to limit $Vcmax_{25}$. Consequently, these results demonstrate that the most accurate reliable means of obtaining $Vcmax_{25}$ from remote sensing data is via Chl_{Leaf}. To improve the statistical confidence in the relationship to produce reliable empirical regressions, data collected during 2015 were also included in the Chl_{Leaf} and $Vcmax_{25}/Jmax_{25}$ regressions (leaf nitrogen data were only collected during 2014).

Figure 6 shows that the different species, whilst exhibiting different ranges and maximum values of Chl_{Leaf} and $Vcmax_{25}/Jmax_{25}$ occupy the same slope, suggesting that a universal equation can be used for multiple species of the same PFT, regardless of differences in biochemistry, leaf structure and photosynthetic rates. The following equations can therefore be taken forward to model $Vcmax_{25}$ and $Jmax_{25}$ from Chl_{Leaf} across larger spatial extents:

$$\mathrm{Vcmax_{25}} = 1.30 \times \mathrm{Chl_{Leaf}}\ (\mu g\,cm^{-2}) + 3.72\ \mu mol\,m^{-2}\,s^{-1} \quad (2)$$

$$\mathrm{Jmax_{25}} = 2.49 \times \mathrm{Chl_{Leaf}}\ (\mu g\,cm^{-2}) + 10.80\ \mu mol\,m^{-2}\,s^{-1} \quad (3)$$

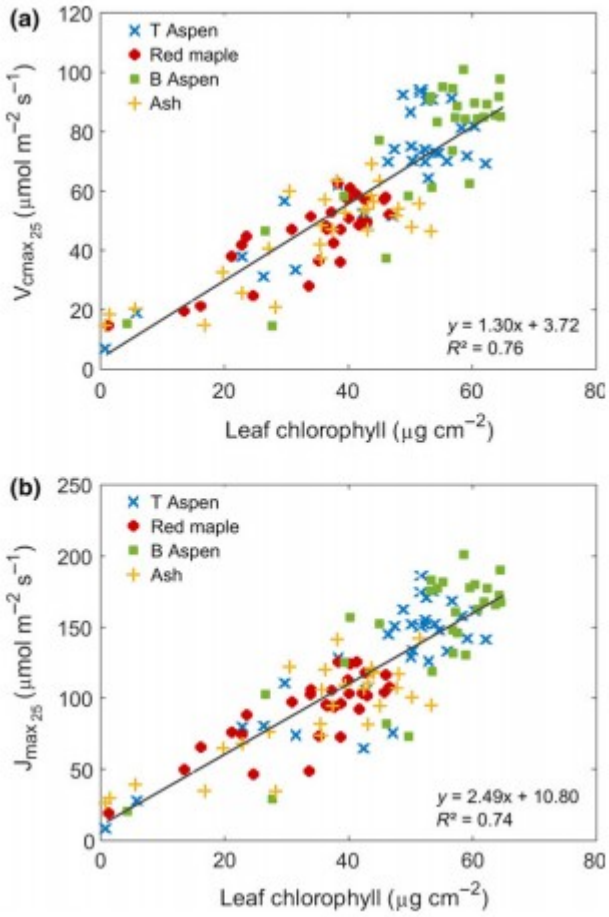

FIGURE 6 Relationships between leaf chlorophyll (µg cm^{-2}) and (a) $V_{cmax_{25}}$ (µmol m^{-2} s^{-1}), $P < 0.001$, and (b) $J_{max_{25}}$ (µmol m^{-2} s^{-1}), $P < 0.001$, for 2014 and 2015 data.

Mapping seasonal variations in $V_{cmax_{25}}$ from satellite-derived reflectance data

To obtain spatially continuous $V_{cmax_{25}}$ values of large spatial extents for input into TBMs, the relationship between Chl_{Leaf} and $V_{cmax_{25}}$ established in Fig. 6a can be employed (Eq. 2). Chl_{Leaf} has been reliably derived from satellite-based reflectance measurements, using radiative transfer models (Croft *et al*., 2013). Figure 7 demonstrates the seasonal relationship between measured and modelled leaf chlorophyll content for three growing seasons (2013–2015), and the overall regression between the two variables. The leaf chlorophyll content shown in Fig. 7 was a weighted average of the four sampled species according to the forest composition (Teklemariam *et al*., 2009). The modelled Chl_{Leaf} values represent all the available cloud-free dates acquired from Landsat satellite images for the Borden Forest.

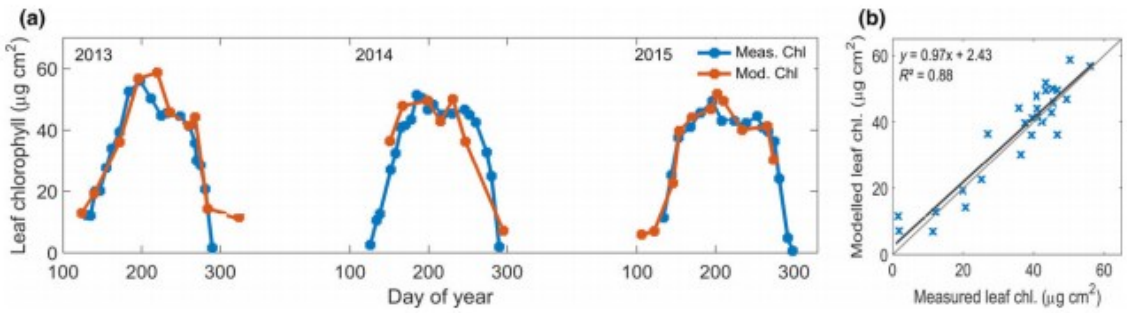

FIGURE 7 The relationship between modelled and measured leaf chlorophyll content over three growing seasons: (a) by date and (b) as an overall regression ($P < 0.001$).

The accuracy of the retrieval of modelled chlorophyll content against measured leaf chlorophyll, in terms of capturing the temporal variation and the overall relationship ($R^2 = 0.88$, $P < 0.01$), demonstrates the choice of using Chl_{Leaf} as a reliable proxy for modelling V_{cmax25} over space and time. It is important not only that the biochemical parameter has a strong relationship with V_{cmax25}, but also that the parameter can be modelled accurately from remotely sensed data.

The spatial variations in V_{cmax25} for the study area are shown at selected dates for the 2015 season, along with a corresponding LAI map for each date (Fig. 8).

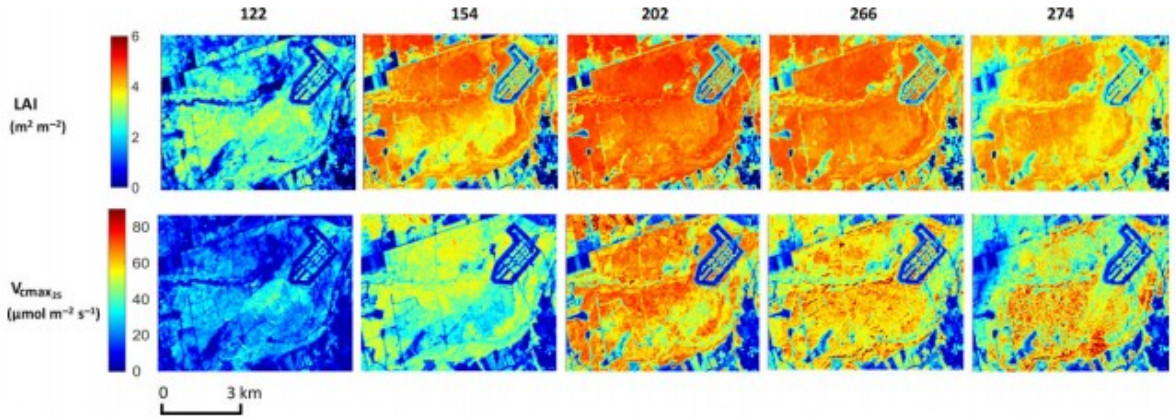

FIGURE 8 Mapped values of LAI (first panel) and V_{cmax25} (second panel) from Landsat satellite data across selected dates (day of year) of the 2015 growing season.

The mapped V_{cmax25} results show considerable temporal and spatial variability across the site, with lower values seen at the start of the growing season, and maximum values in the middle of the season at DOY 202. The decline in V_{cmax25} at the end of the season appears more patchy and fractionated than the start of the season. Higher values are generally seen towards the top portion of the site, with spatial variations likely due to species variability. The LAI maps are shown to demonstrate the deviation between physiology and canopy structure, where LAI is more spatially consistent in the middle of the season (202–266) and also as V_{cmax25} begins

to decline. This also demonstrates the importance in distinguishing overall leaf area from leaf photosynthetic capacity (Croft *et al*., 2014b, 2015a).

Discussion

Impacts of seasonal variations in leaf nitrogen content

It is well established that N_{Leaf} is an important regulator of vegetation productivity and carbon fluxes at a range of spatial scales (LeBauer & Treseder, 2008; Xu *et al*., 2012), and this is because approximately 50% of leaf nitrogen is invested in its photosynthetic apparatus (Niinemets & Sack, 2006). Consequently, many TBMs constrain photosynthetic capacity using fixed relationships between leaf nitrogen content (modulated by nitrogen supply in the soil) and Vcmax (Dietze, 2014). However, the statistical nature of this relationship varies according to a number of environmental conditions, including the light regime, leaf ontogeny, CO_2 concentration and temperature. In contrast to some other studies, who found relatively stable relationships between N_{Leaf} and Vcmax (Ellsworth *et al*., 2004; Kattge *et al*., 2009), this research found weaker correlations between V_{cmax25} and N_{Area} (R^2 = 0.62, $P < 0.001$), which was in large part due to the divergence in the seasonal profile of both variables (Fig. 2), confirming previous studies that found that leaf physiological development continues longer than morphological development (Wilson *et al*., 2001; Xu & Baldocchi, 2003; Croft *et al*., 2014b). The high leaf nitrogen results at the start of the season are due to inorganic N present in buds prior to leaf flushing (Migita *et al*., 2007). During senescence, approximately half the N_{Leaf} content is reabsorbed into storage organs (Migita *et al*., 2007). However, considerable scatter was also found in the middle of the growing season, both within and between different tree species. The partitioning of leaf nitrogen between different fractional pools is dynamic and changes with time and species, according to demand and factors such as growth optimization and environmental drivers (Xu *et al*., 2012). This partitioning involves the distribution of leaf nitrogen among photosynthetic compounds (Hikosaka & Terashima 1998; Hikosaka *et al*. 1996) and also its overall partitioning between photosynthetic and nonphotosynthetic pools (Hikosaka & Terashima 1996; Hikosaka *et al*. 1998). Total N_{Leaf} is not an ideal proxy for photosynthetic capacity directly or through its relationship with Chl_{Leaf}, due to the large and dynamic nitrogen investment in nonphotosynthetic pools, and the changing nitrogen allocation between the RuBisCo and light-harvesting fractions, as a result of different irradiance conditions (Kenzo *et al*., 2006). This has important implications for remote sensing approaches focussed on modelling N_{Leaf} directly or using N_{Leaf} as an intermediary (Houborg *et al*., 2015). Previous studies have reported that nitrogen is a relatively constant fraction of Chl_{Leaf}, with Chl_{Leaf}/N_{Leaf} ratios of 3.8 ± 0.3 for agricultural species of different photosynthetic pathways (Field & Mooney, 1986; Sage *et al*., 1987; Houborg *et al*., 2013). Our results demonstrated that this constant 3.8 ratio was reasonable in the middle of the growing season for two sunlit deciduous species (red maple and ash), although values were 3.1 and 3.0 for Trembling and bigtooth aspen,

respectively. However, Chl_{Leaf}/N_{Leaf} ratios at the start of season were much lower, with minimum values ranging from 0.8 for red maple to 1.2 for ash and aspen, with lower ratios also seen at the end of the season.

Physiological basis for leaf chlorophyll as a proxy for photosynthetic capacity

The results in this study demonstrate that it is more accurate to use Chl_{Leaf} to model $Vcmax_{25}$ directly, rather than via N_{Area}. This also reduces the additional error associated with the Chl_{Leaf}-N_{Area} relationship ($R^2 = 0.47$), $P < 0.001$, when Chl_{Leaf} is used as an intermediary in remote sensing approaches, due to the difficulty in obtaining N_{Area} directly. The direct use of Chl_{Leaf} also has a physiological basis, due to the inherent dependence of photosynthesis on chlorophyll molecules as the primary means of harvesting light energy to drive the electron transport reactions. The first stage in photosynthesis is the absorption of light energy by chlorophyll molecules embedded in the thylakoid membranes of chloroplasts. Light quanta harvested by chlorophyll molecules in Photosystem II provides the energy to supply electrons, through the electron transport chain to Photosystem I via the cytochrome b_6f complex, to produce NADPH and chemical energy as ATP for the reactions of the Calvin–Benson cycle. The amount of light absorbed by a leaf has been shown to be related to Chl_{Leaf} across a number of different plant species (Evans, 1996; Evans & Poorter, 2001), with the potential rate of electron transport J (μmol electrons $m^{-2}\,s^{-1}$) in turn dependent on leaf-absorbed PAR (ϕ; μmol photons $m^{-2}\,s^{-1}$), according to the following:

$$0.7J^2 - (\mathrm{Jmax} + 0.385\Phi)J + 0.385\mathrm{Jmax}\Phi = 0 \quad (4)$$

The rate of electron transport is therefore a function of incident PAR and the efficiency of a leaf's light-harvesting apparatus (i.e. chlorophyll) (Collatz *et al*., 1991; Sellers *et al*., 1992). Therefore, whilst Chl_{Leaf} is theoretically more closely related to $Jmax_{25}$ than to $Vcmax_{25}$ which is proportional to leaf RuBisCo content (Bonan, 2015), a consistent linear relationship between $Jmax_{25}$ and $Vcmax_{25}$ is found across a large range of species (Medlyn *et al*., 2002). Experimentally, Singsaas *et al*. (2004) also demonstrated that RuBP regeneration capacity increased linearly with total leaf chlorophyll content.

Towards mapping $Vcmax_{25}$ at global scales

The results presented in this study indicate that Chl_{Leaf} has strong potential to be used as a proxy for photosynthetic capacity and provide spatially explicit $Vcmax_{25}$ maps for incorporation into global TBMs. The use of Chl_{Leaf} removes the need for empirical corrections according to leaf ontogeny for N–Vcmax relationships proposed when using N_{Area} in TBMs (Wilson *et al*., 2001; Grassi *et al*., 2005). It is recognized that this approach has only been demonstrated at a mixed deciduous forest site and needs to be investigated in other ecosystems, with different species assemblages, nutrient supply, light conditions, temperature ranges and moisture availability. The use of Chl_{Leaf}, over N_{Area} in particular, is especially valuable in being able to capture seasonal trends in $Amax_{400}$, and also $Vcmax_{25}/Jmax_{25}$, which may correct

start/end of season overestimations in modelled GPP values (Croft *et al*., 2015a). An alternative remote sensing approach for producing V_{cmax25} spatial products is through the use of solar-induced chlorophyll fluorescence (Zhang *et al*., 2014). Whilst these techniques are promising, measurements are only typically available at very coarse spatial resolutions (i.e. GOME-2 – 40 × 80 km^2), compared to optical sensors which typically operate in the decametre to hectometre range. A significant operational limitation to parameterizing V_{cmax25} using Chl_{Leaf} at large spatial scales is the absence of accurate Chl_{Leaf} products at regional or global scales, which has largely been hampered by a lack of satellite sensors sampling over chlorophyll-sensitive wavelengths (predominately 'red-edge bands'). At local scales, modelled Chl_{Leaf} results have shown some success using empirical vegetation indices (Wu *et al*., 2008); however, the empirical nature of these relationships means that they have been difficult to apply over larger spatial extents, time intervals and different species (Croft *et al*., 2014c). The inversion of physically based radiative transfer models (Zhang *et al*., 2008; Houborg *et al*., 2009; Croft *et al*., 2013) has shown potential for applying these techniques over broader spatial scales and also using a reduced number of spectral bands (Croft *et al*., 2015b). Thus, the prospect of obtaining spatially distributed chlorophyll measurements across global scales is becoming more achievable.

Implications for global terrestrial biosphere modelling

Thus far, TBMs have largely treated photosynthetic parameters as either fixed constants or varying according to empirical relationships with N_{Leaf}. However, this paper has challenged the assumptions that 1) total leaf nitrogen data (both by N_{Mass} and N_{Area}) are reliable parameters in constraining V_{cmax25} within TBMs, even within the same functional type, and 2) that Chl_{Leaf} can be used to accurately retrieve N_{Leaf} for application over large spatial scales. This research particularly emphasizes the confounding influence of temporal and species-specific variations of nitrogen contained in structural fractions and highlights the necessity of quantitatively specifying the relevant nitrogen pool rather than using total N_{Leaf}. This identifies a knowledge gap with respect to current implementations of a nitrogen cycle in TBMs wherein N_{Leaf} is used to limit V_{cmax25} without accounting for its partitioning to photosynthetic and structural components, the controls of which are not yet fully realized. The following findings are important contributions for improving the accuracy of modelled carbon exchange within global terrestrial models:

1. Total nitrogen content is not an accurate proxy for V_{cmax25} (N_{Area}, R^2 = 0.62; $P < 0.001$) particularly in a seasonal context where large variations in V_{cmax25} exist. Whilst nitrogen fractions invested in photosynthetic proteins (i.e. RuBisCo nitrogen) may show a strong relationship with V_{cmax25}, instead it is more accurate to use Chl_{Leaf} directly to model V_{cmax25} (R^2 = 0.76; $P < 0.001$), which also reduces the additional error associated with the Chl_{Leaf}–N_{Area} relationship (R^2 =

0.47; $P < 0.001$) and does not require corrections for variations in leaf structure.

2. The relationship between leaf chlorophyll content and total leaf nitrogen (N_{Area}, $R^2 = 0.47$; $P < 0.001$; N_{Mass}, $R^2 = 0.10$; $P < 0.001$) is complex and subject to several sources of variability, including the dynamic partitioning of nitrogen between photosynthetic and nonphotosynthetic pools, and also within the different photosynthetic fractions, for example, due to changing illumination conditions. This result has large implications for remote sensing research, which has faced difficulty directly retrieving leaf nitrogen due to the absence of strong spectral absorption features compared to Chl_{Leaf} and instead often derives leaf nitrogen content from relationships with Chl_{Leaf}.
3. V_{cmax25} shows considerable variability across a growing season, and between plant species, even within the same plant functional type. This result confirms previous suggestions that using a fixed V_{cmax25} value within TBMs is likely to lead to large errors in modelled photosynthesis within ecosystems with a large seasonal range in photosynthetic capacity. Further, it confirms that it is also not adequate to fix V_{cmax25} values for given plant functional types and that spatially and temporally continuous V_{cmax25} estimates are needed to increase the reliability of carbon balance predictions under current and future climate scenarios.

References

Beer C, Reichstein M, Tomelleri E *et al*. (2010) Terrestrial gross carbon dioxide uptake: global distribution and covariation with climate. *Science*, 329, 834– 838.

Bonan G (2015) *Ecological Climatology: Concepts and Applications*. Cambridge University Press, New York.

Brienen RJW, Phillips OL, Feldpausch TR *et al*. (2015) Long-term decline of the Amazon carbon sink. *Nature*, 519, 344– 348.

von Caemmerer S, Farquhar GD (1981) Some relationships between the biochemistry of photosynthesis and the gas exchange of leaves. *Planta*, 153, 376– 387.

Chen JM, Cihlar J (1995) Plant canopy gap-size analysis theory for improving optical measurements of leaf-area index. *Applied Optics*, 34, 6211– 6222.

Chen JM, Leblanc SG (1997) A four-scale bidirectional reflectance model based on canopy architecture. *IEEE Transactions on Geoscience and Remote Sensing*, 35, 1316– 1337.

Chen JM, Leblanc SG (2001) Multiple-scattering scheme useful for geometric optical modeling. *IEEE Transactions on Geoscience and Remote Sensing*, 39, 1061– 1071.

Chen JM, Plummer PS, Rich M, Gower ST, Norman JM (1997) Leaf area index measurements. *Journal of Geophysical Research*, 102, 29– 429.

Collatz GJ, Ball JT, Grivet C, Berry JA (1991) Physiological and environmental regulation of stomatal conductance, photosynthesis and transpiration: a model that includes a laminar boundary layer. *Agricultural and Forest Meteorology*, 54, 107– 136.

Croft H, Chen JM, Zhang Y, Simic A (2013) Modelling leaf chlorophyll content in broadleaf and needle leaf canopies from ground, CASI, Landsat TM 5 and MERIS reflectance data. *Remote Sensing of Environment*, 133, 128– 140.

Croft H, Chen J, Noland T (2014a) Stand age effects on Boreal forest physiology using a long time-series of satellite data. *Forest Ecology and Management*, 328, 202– 208.

Croft H, Chen JM, Zhang Y (2014b) Temporal disparity in leaf chlorophyll content and leaf area index across a growing season in a temperate deciduous forest. *International Journal of Applied Earth Observation and Geoinformation*, 33, 312– 320.

Croft H, Chen JM, Zhang Y (2014c) The applicability of empirical vegetation indices for determining leaf chlorophyll content over different leaf and canopy structures. *Ecological Complexity*, 17, 119– 130.

Croft H, Chen J, Froelich N, Chen B, Staebler R (2015a) Seasonal controls of canopy chlorophyll content on forest carbon uptake: Implications for GPP modeling. *Journal of Geophysical Research: Biogeosciences*, 120, 1576– 1586.

Croft H, Chen J, Zhang Y, Simic A, Noland T, Nesbitt N, Arabian J (2015b) Evaluating leaf chlorophyll content prediction from multispectral remote sensing data within a physically-based modelling framework. *ISPRS Journal of Photogrammetry and Remote Sensing*, 102, 85– 95.

Dietze MC (2014) Gaps in knowledge and data driving uncertainty in models of photosynthesis. *Photosynthesis Research*, 119, 3– 14.

Dillen SY, de Beeck MO, Hufkens K, Buonanduci M, Phillips NG (2012) Seasonal patterns of foliar reflectance in relation to photosynthetic capacity and color index in two co-occurring tree species, *Quercus rubra* and *Betula papyrifera*. *Agricultural and Forest Meteorology*, 160, 60– 68.

Ellsworth DS, Reich PB, Naumburg ES, Koch GW, Kubiske ME, Smith SD (2004) Photosynthesis, carboxylation and leaf nitrogen responses of 16 species to elevated pCO_2 across four free-air CO_2 enrichment experiments in forest, grassland and desert. *Global Change Biology*, 10, 2121– 2138.

Ethier G, Livingston N (2004) On the need to incorporate sensitivity to CO_2 transfer conductance into the Farquhar–von Caemmerer-Berry leaf photosynthesis model. *Plant, Cell & Environment*, 27, 137– 153.

Evans JR (1996) Developmental constraints on photosynthesis: effects of light and nutrition. In: *Photosynthesis and the Environment* (ed. NR Baker), pp. 281– 304. Kluwer, Dordrecht.

Evans J, Poorter H (2001) Photosynthetic acclimation of plants to growth irradiance: the relative importance of specific leaf area and nitrogen partitioning in maximizing carbon gain. *Plant, Cell & Environment*, 24, 755–767.

Farquhar GD, von Caemmerer S, Berry JA (1980) A biochemical model of photosynthetic CO_2 assimilation in leaves of C3 species. *Planta*, 149, 78– 90.

Field C, Mooney HA (1986) The photosynthesis–nitrogen relationship in wild plants. In: *On the Economy of Plant Form and Function* (ed. TJ Givnish), pp. 25– 55. Cambridge University Press, Cambridge.

Froelich N, Croft H, Chen JM, Gonsamo A, Staebler R (2015) Trends of carbon fluxes and climate over a mixed temperate–boreal transition forest in southern Ontario, Canada. *Agricultural and Forest Meteorology*, 211, 72– 84.

Gitelson AA, Viña A, Verma SB *et al*. (2006) Relationship between gross primary production and chlorophyll content in crops: Implications for the synoptic monitoring of vegetation productivity. *Journal of Geophysical Research D: Atmospheres*, 111.

Gower ST, Kucharik CJ, Norman JM (1999) Direct and indirect estimation of leaf area index, f(APAR), and net primary production of terrestrial ecosystems. *Remote Sensing of Environment*, 70, 29– 51.

Grassi G, Vicinelli E, Ponti F, Cantoni L, Magnani F (2005) Seasonal and interannual variability of photosynthetic capacity in relation to leaf nitrogen in a deciduous forest plantation in northern Italy. *Tree Physiology*, 25, 349–360.

Groenendijk M, Dolman AJ, van der Molen MK *et al*. (2011) Assessing parameter variability in a photosynthesis model within and between plant functional types using global Fluxnet eddy covariance data. *Agricultural and Forest Meteorology*, 151, 22– 38.

Hikosaka K, Hanba YT, Hirose T, Terashima I (1998) Photosynthetic nitrogen-use efficiency in leaves of woody and herbaceous species. *Functional Ecology*, 12, 896– 905.

Hikosaka K, Terashima I (1996) Nitrogen partitioning among photosynthetic components and its consequence in sun and shade plants. *Functional Ecology*, 10, 335– 343.

Hilker T, Coops NC, Wulder MA, Black TA, Guy RD (2008) The use of remote sensing in light use efficiency based models of gross primary production: a review of current status and future requirements. *Science of the Total Environment*, 404, 411– 423.

Homolova L, Malenovský Z, Clevers JG, Garcia-Santos G, Schaepman ME (2013) Review of optical-based remote sensing for plant trait mapping. *Ecological Complexity*, 15, 1– 16.

Houborg R, Anderson M, Daughtry C (2009) Utility of an image-based canopy reflectance modeling tool for remote estimation of LAI and leaf chlorophyll content at the field scale. *Remote Sensing of Environment*, 113, 259– 274.

Houborg R, Cescatti A, Migliavacca M, Kustas W (2013) Satellite retrievals of leaf chlorophyll and photosynthetic capacity for improved modeling of GPP. *Agricultural and Forest Meteorology*, 177, 10– 23.

Houborg R, McCabe MF, Cescatti A, Gitelson AA (2015) Leaf chlorophyll constraint on model simulated gross primary productivity in agricultural systems. *International Journal of Applied Earth Observation and Geoinformation*, 43, 160– 176.

IPCC (2013). Climate Change 2013: The Physical Science Basis. Contribution of Working Group I to the Fifth Assessment Report of the Intergovernmental Panel on Climate Change. In: (eds Stock TF, Qin D, Plattner G-K, Tignor M, Allen S, Boschung J, Nauels A, Xia Y, Bex V, & Midgley P), p. 1535. Cambridge, UK & New York, NY, USA.

Jacquemoud S, Baret F (1990) PROSPECT: a model of leaf optical properties spectra. *Remote Sensing of Environment*, 34, 75– 91.

Joiner J, Yoshida Y, Vasilkov A, Middleton E (2011) First observations of global and seasonal terrestrial chlorophyll fluorescence from space. *Biogeosciences*, 8, 637– 651.

Kattge J, Knorr W, Raddatz T, Wirth C (2009) Quantifying photosynthetic capacity and its relationship to leaf nitrogen content for global-scale terrestrial biosphere models. *Global Change Biology*, 15, 976– 991.

Kenzo T, Ichie T, Watanabe Y, Yoneda R, Ninomiya I, Koike T (2006) Changes in photosynthesis and leaf characteristics with tree height in five dipterocarp species in a tropical rain forest. *Tree Physiology*, 26, 865– 873.

Knyazikhin Y, Schull MA, Stenberg P *et al*. (2013) Hyperspectral remote sensing of foliar nitrogen content. *Proceedings of the National Academy of Sciences*, 110, E185– E192.

LeBauer DS, Treseder KK (2008) Nitrogen limitation of net primary productivity in terrestrial ecosystems is globally distributed. *Ecology*, 89, 371– 379.

Lee X, Fuentes JD, Staebler RM, Neumann HH (1999) Long-term observation of the atmospheric exchange of CO2 with a temperate deciduous forest in southern Ontario, Canada. *Journal of Geophysical Research: Atmospheres*, 104, 15975– 15984.

Leithead M, Anand M, Silva LR (2010) Northward migrating trees establish in treefall gaps at the northern limit of the temperate–boreal ecotone, Ontario, Canada. *Oecologia*, 164, 1095– 1106.

Medlyn B, Dreyer E, Ellsworth D *et al*. (2002) Temperature response of parameters of a biochemically based model of photosynthesis. II. A review of experimental data. *Plant, Cell & Environment*, 25, 1167– 1179.

Medvigy D, Jeong S-J, Clark KL, Skowronski NS, Schäfer KVR (2013) Effects of seasonal variation of photosynthetic capacity on the carbon fluxes of a temperate deciduous forest. *Journal of Geophysical Research: Biogeosciences*, 118, 1703– 1714.

Migita C, Chiba Y, Tange T (2007) Seasonal and spatial variations in leaf nitrogen content and resorption in a *Quercus serrata* canopy. *Tree Physiology*, 27, 63– 70.

Niinemets U, Sack L (2006) Structural determinants of leaf light-harvesting capacity and photosynthetic potentials. *Progress in Botany*, 67, 385– 419.

Niinemets Ü, Tenhunen JD (1997) A model separating leaf structural and physiological effects on carbon gain along light gradients for the shade-tolerant species *Acer saccharum*. *Plant, Cell and Environment*, 20, 845– 866.

Pan Y, Birdsey RA, Fang J *et al*. (2011) A large and persistent carbon sink in the world's forests. *Science*, 333, 988– 993.

Sage RF, Pearcy RW, Seemann JR (1987) The nitrogen use efficiency of C3 and C4 plants III. Leaf nitrogen effects on the activity of carboxylating enzymes in *Chenopodium album* (L.) and *Amaranthus retroflexus* (L.). *Plant Physiology*, 85, 355– 359.

Schull M, Anderson M, Houborg R, Gitelson A, Kustas W (2015) Thermal-based modeling of coupled carbon, water, and energy fluxes using nominal light use efficiencies constrained by leaf chlorophyll observations. *Biogeosciences*, 12, 1511– 1523.

Sellers P, Berry J, Collatz G, Field C, Hall F (1992) Canopy reflectance, photosynthesis, and transpiration. III. A reanalysis using improved leaf models and a new canopy integration scheme. *Remote Sensing of Environment*, 42, 187– 216.

Serbin SP, Singh A, Desai AR *et al*. (2015) Remotely estimating photosynthetic capacity, and its response to temperature, in vegetation canopies using imaging spectroscopy. *Remote Sensing of Environment*, 167, 78– 87.

Sharkey TD (2016) What gas exchange data can tell us about photosynthesis. *Plant, Cell & Environment*, 39, 1161– 1163.

Sharkey TD, Bernacchi CJ, Farquhar GD, Singsaas EL (2007) Fitting photosynthetic carbon dioxide response curves for C3 leaves. *Plant, Cell & Environment*, 30, 1035– 1040.

Singsaas E, Ort D, DeLucia E (2004) Elevated CO_2 effects on mesophyll conductance and its consequences for interpreting photosynthetic physiology. *Plant, Cell & Environment*, 27, 41– 50.

Teklemariam T, Staebler RM, Barr AG (2009) Eight years of carbon dioxide exchange above a mixed forest at Borden, Ontario. *Agricultural and Forest Meteorology*, 149, 2040– 2053.

Turner DP, Urbanski S, Bremer D, Wofsy SC, Meyers T, Gower ST, Gregory M (2003) A cross-biome comparison of daily light use efficiency for gross primary production. *Global Change Biology*, 9, 383– 395.

Walker AP, Beckerman AP, Gu L *et al*. (2014) The relationship of leaf photosynthetic traits–Vcmax and Jmax–to leaf nitrogen, leaf phosphorus, and specific leaf area: a meta-analysis and modeling study. *Ecology and Evolution*, 4, 3218– 3235.

Wang YP, Baldocchi D, Leuning RAY, Falge EVA, Vesala T (2007) Estimating parameters in a land-surface model by applying nonlinear inversion to eddy covariance flux measurements from eight FLUXNET sites. *Global Change Biology*, 13, 652– 670.

Wellburn AR (1994) The spectral determination of chlorophylls a and b, as well as total carotenoids, using various solvents with spectrophotometers of different resolution. *Journal of Plant Physiology*, 144, 307– 313.

Wilson K, Baldocchi D, Hanson P (2001) Leaf age affects the seasonal pattern of photosynthetic capacityand net ecosystem exchange of carbon in a deciduous forest. *Plant, Cell & Environment*, 24, 571– 583.

Wu C, Niu Z, Tang Q, Huang W (2008) Estimating chlorophyll content from hyperspectral vegetation indices: Modeling and validation. *Agricultural and Forest Meteorology*, 148, 1230– 1241.

Xu L, Baldocchi DD (2003) Seasonal trends in photosynthetic parameters and stomatal conductance of blue oak (*Quercus douglasii*) under prolonged summer drought and high temperature. *Tree Physiology*, 23, 865– 877.

Xu C, Fisher R, Wullschleger SD, Wilson CJ, Cai M, McDowell NG (2012) Toward a mechanistic modeling of nitrogen limitation on vegetation dynamics. *PLoS One*, 7, e37914.

Zhang Y, Chen JM, Thomas SC (2007) Retrieving seasonal variation in chlorophyll content of overstory and understory sugar maple leaves from leaf-level hyperspectral data. *Canadian Journal of Remote Sensing*, 33, 406–415.

Zhang Y, Chen JM, Miller JR, Noland TL (2008) Leaf chlorophyll content retrieval from airborne hyperspectral remote sensing imagery. *Remote Sensing of Environment*, 112, 3234– 3247.

Zhang Y, Guanter L, Berry JA *et al*. (2014) Estimation of vegetation photosynthetic capacity from space-based measurements of chlorophyll

fluorescence for terrestrial biosphere models. *Global Change Biology*, 20, 3727– 3742.